

## Review Article

# Silicon-Based Light Sources for Silicon Integrated Circuits

L. Pavesi

*Nanoscience Laboratory, Department of Physics, University of Trento, 38050 Povo, Trento, Italy*

Correspondence should be addressed to L. Pavesi, [pavesi@science.unitn.it](mailto:pavesi@science.unitn.it)

Received 15 January 2008; Accepted 30 April 2008

Recommended by D. Lockwood

Silicon the material per excellence for electronics is not used for sourcing light due to the lack of efficient light emitters and lasers. In this review, after having introduced the basics on lasing, I will discuss the physical reasons why silicon is not a laser material and the approaches to make it lasing. I will start with bulk silicon, then I will discuss silicon nanocrystals and  $\text{Er}^{3+}$  coupled silicon nanocrystals where significant advances have been done in the past and can be expected in the near future. I will conclude with an optimistic note on silicon lasing.

Copyright © 2008 L. Pavesi. This is an open access article distributed under the Creative Commons Attribution License, which permits unrestricted use, distribution, and reproduction in any medium, provided the original work is properly cited.

## 1. INTRODUCTION

Recently, a large research effort has been dedicated to the development of compact optoelectronic platforms. The increasing interest in conjugating optical functionality to integrated circuits stems not only from the potential of optics to overcome interconnect bottlenecks imposed on electronic circuits by speed, power, and space demands, but also from their flexibility for human interface devices (e.g., displays and image recognition) and for a large set of specific applications (including, e.g., biological sensors and compact optical tomography apparatus). Optical signals are generally interesting in connection to low power consumption, a key issue in the context of general trends such as increased miniaturization and wireless and autonomous operation.

From the industrial perspective, the preferred route towards optoelectronic platforms is the upgrade of existing electronic technology, in which Si has had no competitors since the 1960's. Compared to Ge, Si has larger bandgap (1.12 eV), which allows higher operating temperature, can be naturally structured with a companion insulator ( $\text{SiO}_2$ ), and is cheap and easily available. On the other hand, compound semiconductor technologies, such as InP or GaAs, are not competitive with Si essentially because of cost issues.

While monolithic Si-compatible solutions have been known since several years for many devices such as light detectors, waveguides, and modulators, the lack of monolithic energy-efficient and cost-effective CMOS-compatible light sources has hampered the development of optoelectronic and photonic platforms. In this paper, we consider

the state of the art of Si-based light-emitting devices for Si integrated circuits. The reader is encouraged to consult also the various review articles or books which have been published on the topic of light emission in Si [1–8] as well as on hybrid technology [9]. It is worth to note that in this paper we will not discuss the hybrid approach based on III–V semiconductors either bonded or heteroepitaxied on silicon, though hybrid lasers have been integrated in silicon with very promising performances.

## 2. BASICS OF LIGHT AMPLIFICATION AND GAIN

A laser requires three main components: an active material which is able to generate and amplify light by stimulated emission of photons, an optical cavity which provides the optical feedback to sustain the laser action, and a pumping mechanism to supply energy to the active material. In the case of lasers based on first-order optical processes, the pumping mechanism must be able to produce a population inversion in the material. In an injection diode laser, the pumping mechanism is provided by carrier injection via a p-n junction and the optical feedback is usually provided by a Fabry-Perot cavity, [10, 11] although recently whispering gallery resonators (microdisks) and photonic crystals are receiving increasing attention.

The light generation by electron-hole recombination in semiconductors is quantified by the internal quantum efficiency  $\eta_{\text{int}}$ , which is the ratio between the number of generated photons and the number of electron-hole pairs that

recombine. This number is given by the ratio of the electron-hole (e-h) radiative recombination probability over the total e-h recombination probability, that is, by the fraction of all excited e-h pairs that recombine radiatively. It is easy to demonstrate that  $\eta_{\text{int}} = \tau_{nr}/(\tau_{nr} + \tau_r)$ , where  $\tau_{nr}$  and  $\tau_r$  are the nonradiative and radiative lifetimes, respectively. Thus, in order to have a high  $\eta_{\text{int}}$ , either the radiative lifetime should be short (as in direct bandgap semiconductors) or the nonradiative lifetime should be long (as in color center systems).

The property of amplifying light is given by the gain spectrum of the material. For a bulk semiconductor, it is related to the joint density of states  $\rho(\hbar\omega)$ , the Fermi inversion factor  $f_g(\hbar\omega)$ , and the radiative lifetime:

$$\begin{aligned} d\Phi(\hbar\omega) &= dr_{\text{stim}}(\hbar\omega) - dr_{\text{abs}}(\hbar\omega) \\ &= \frac{\lambda^2}{8\pi\tau_r} \rho(\hbar\omega) f_g(\hbar\omega) \Phi(\hbar\omega) dz \\ &= g(\hbar\omega) \Phi(\hbar\omega) dz, \end{aligned} \quad (1)$$

where  $g(\hbar\omega)$  is the gain coefficient,  $d\Phi$  is the change in the photon flux,  $dr_{\text{stim}}$  or  $dr_{\text{abs}}$  is the rate of stimulated emission or absorption at a given photon energy  $\hbar\omega$ , respectively,  $f_g(\hbar\omega, E_F^e, E_F^h, T) = [f_e(\hbar\omega, E_F^e, T) - (1 - f_h(\hbar\omega, E_F^h, T))]$ ,  $f_e$  and  $f_h$  are the thermal occupation functions for electrons and holes, and  $\Phi$  is the photon flux density.  $E_F^e$  and  $E_F^h$  are the quasi-Fermi levels for electrons and holes, respectively. When no external pumping is present, the Fermi inversion factor reduces to the simple Fermi statistics for an empty conduction band and a filled valence band ( $f_g < 0$ ), and the gain coefficient reduces to the absorption coefficient  $\alpha$ . When an external pump excites a large density of free carriers, the splitting of the quasi-Fermi levels increases, and when  $E_F^e - E_F^h > \hbar\omega$  the condition of population inversion is satisfied and  $f_g > 0$ . This means that (1) is positive and hence the system shows positive net optical gain ( $g > 0$ ). Note that in (1) a critical role is played by the radiative lifetime: the shorter the lifetime, the stronger the gain.

For an atomic system, the expression of the gain coefficient reduces to

$$g(\hbar\omega) = \sigma_{\text{em}}(\hbar\omega)N_2 - \sigma_{\text{abs}}(\hbar\omega)N_1, \quad (2)$$

where  $\sigma_{\text{em}}$  is the emission cross-section,  $\sigma_{\text{abs}}$  is the absorption cross-section, and  $N_2$  and  $N_1$  represent the density of active centers in the excited and ground states, respectively. If  $\sigma_{\text{em}} = \sigma_{\text{abs}}$ , the condition to have positive optical gain is that  $N_2 > N_1$ , that is, the condition of population inversion.

If a piece of active material of length  $L$  is used to amplify light, one achieves light amplification whenever the material gain  $g$  is positive and larger than the propagation losses  $\alpha_p$  of the light through the material, that is,  $g > 0$  and  $g > \alpha_p$ . If the system is forged as a waveguide of length  $L$ , and we call  $I_T$  and  $I_0$  the intensity of the transmitted and the incident beams, the amplification factor of the light is then

$$G = \frac{I_T}{I_0} = \exp[(\Gamma g - \alpha_p)L] > 1, \quad (3)$$

where  $\Gamma$  is the optical confinement factor of the optical mode in the active region.

In a laser, optical feedback is usually provided by a Fabry-Perot cavity so that the round-trip gain (the overall gain experienced by a photon traveling back and forth across the cavity) can be larger than 1. This condition is expressed by the relation  $G^2 R_1 R_2 > 1$ , where  $R_1$  and  $R_2$  are the back and front mirror reflectivities.

### 3. LIMITATION OF Si FOR LIGHT EMISSION AND AMPLIFICATION

Among the various semiconductor materials which have been used to form LEDs and lasers, the absence of Si is striking. Let us review why Si has not been used as a light-emitting material [4, 5, 7, 8]. Si is an indirect bandgap semiconductor (see Figure 1). As a consequence, the probability for a radiative recombination is low, which in turn means that the e-h radiative lifetime is long (of the order of some milliseconds). An e-h pair has to wait on average a few milliseconds to recombine radiatively. During this time, both the electron and the hole move around and cover a volume of the order of  $10 \mu\text{m}^3$ . If they encounter a defect or a trapping center, the carriers might recombine nonradiatively. Typical nonradiative recombination lifetimes in Si are of the order of some nanoseconds. Thus, in electronic grade Si, the internal quantum efficiency  $\eta_{\text{int}}$  is about  $10^{-6}$ . This is the reason why Si is a poor luminescent material, that is, the efficient nonradiative recombinations which rapidly deplete the excited carriers. Many strategies have been researched over the years to overcome this Si limitation, and some of which are based on the spatial confinement of the carriers, and others on the introduction of impurities, the use of quantum confinement, and the use of Si-Ge alloys or superlattices [4]. The fact that a slow emission, that is, a long radiative lifetime, is also associated with low brightness of the source and with the requirement of an external modulation scheme for high-speed data transmission is to be noticed.

In addition, two other phenomena limit the use of Si for optical amplification (see Figure 1). The first is a non-radiative three-particle recombination mechanism where an excited electron (hole) recombines with a hole (electron) by releasing the excess energy to another electron (hole). This is called nonradiative Auger recombination mechanism (Figure 1). This recombination mechanism is active as soon as more than one carrier is excited. The probability of an Auger recombination is proportional to the square of the number of excited carriers  $\Delta n$  and inversely proportional to the bandgap energy [12]. For our discussion, this is a very relevant mechanism because the more excited the semiconductor is, the more the Auger recombination is effective. The probability for an Auger recombination in a bulk material is proportional to  $\Delta n^2$ ; we can thus write a nonradiative recombination lifetime due to Auger as  $\tau_A = 1/C\Delta n^2$ , where  $C$  is a constant which depends on the doping of the material. For Si  $C \sim 10^{-30} \text{cm}^6 \text{s}^{-1}$  [7]. For  $\Delta n \sim 10^{19} \text{cm}^3$ ,  $\tau_A = 10$  nanoseconds. The Auger recombination is the dominant recombination mechanism for high carrier injection rate in Si.

The second phenomenon is related to free-carrier absorption (see Figure 1). Excited carriers might absorb photons and thus deplete the inverted population and, at

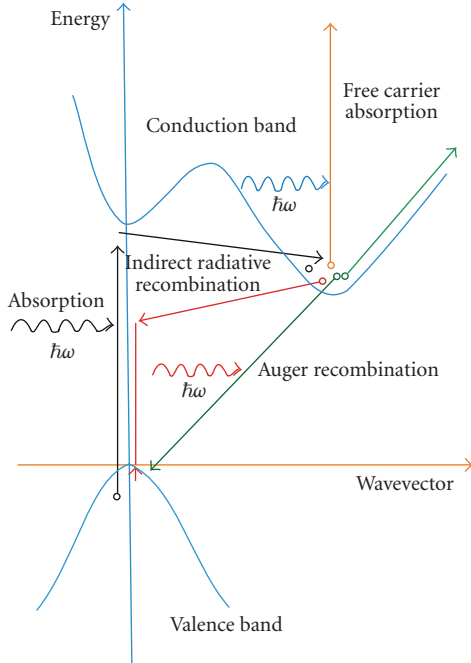


FIGURE 1: Band structure of bulk Si with the various possible transitions for an electron-hole pair: radiative recombination, Auger recombination, and free-carrier absorption.

the same time, increase the optical losses suffered by the signal beam. The free-carrier absorption coefficient can be empirically related to the Si free-carrier density  $n_{fc}$  and to the light wavelength  $\lambda$  as  $\alpha_n \sim 10^{-18} n_{fc} \lambda^2$  at 300 K [7]. For  $n_{fc} = 10^{19} \text{ cm}^{-3}$  and  $\lambda = 1.55 \mu\text{m}$ ,  $\alpha_n = 24 \text{ cm}^{-1}$ . For heavily doped Si, these are the main limitations to lasing, while for intrinsic Si this contribution can be exceedingly small unless  $n_{fc}$  is very high as in a laser. In confined systems, such as Si nanocrystals, this recombination mechanism is due to confined carriers, and hence it is called confined carrier absorption.

#### 4. APPROACHES TO SI LIGHT-EMITTING SOURCES

In early 2000's, a series of papers appeared, which questioned the common belief that Si cannot be used to form a laser [13–19]. In October 2004, the first report on an Si laser appeared [20–22], while in February 2005 the first CW Raman laser integrated in Si was reported [23–25]. Hybrid approaches became effective in 2006–2007 [9]. We summarize the most relevant approaches towards light emission in Si in the following list.

*High-quality bulk Si inserted in a forward biased solar cell.* This approach has a demonstrated emission wavelength of  $1.1 \mu\text{m}$ , and its system features include LED. The advantages of such approach are demonstrated through a power efficiency of  $>1\%$  at 200 K and through the highly efficient electrical injection, and the disadvantages are demonstrated by a wavelength in an unsuitable wavelength region.

Evidence of optical gain has never been reported in Si [15, 26].

*Stimulated Raman scattering in Si waveguides.* The demonstrated emission wavelength of such system is  $1.6 \mu\text{m}$ , and its system features include CW optically pumped Raman laser. Its advantages are demonstrated by the fact that it is the only system where lasing has been clearly demonstrated in a cavity, and the continuously tunable wavelength in near infrared. The disadvantage is that no electrical injection is achievable according to fundamental mechanism [24, 25].

*Nanopatterned Si.* The demonstrated emission wavelength of the system is  $1.28 \mu\text{m}$ , and its system features include optically pumped stimulated emission at cryogenic temperature. The advantages include significant line narrowing and threshold behaviour at low pumping power, and the disadvantages are manifested by a wavelength in an unsuitable wavelength region, and the fact that the effect is demonstrated only at cryogenic temperature and that electrical injection seems prohibitive [16].

*Dislocation loops formed by ion implantation in an Si p-n junction.* The demonstrated emission wavelength is  $1.1 \mu\text{m}$ . The system features include LED with a significant efficiency. The advantages are demonstrated through simple fabrication method and efficient electrical injection, and the disadvantages through a wavelength in an unsuitable wavelength region. The evidence of optical gain has never been reported in Si [27].

*Si nanocrystals in dielectric (SiO<sub>2</sub>) matrix.* The system's demonstrated emission wavelength is  $0.75 \mu\text{m}$ , and its system features include optical gain at room temperature and efficient LED demonstrated in AC electrical pumping regime. The advantages lie in the fact that it is CMOS-compatible and easy to fabricate, as well as its demonstrated optical microcavity and electrical injection scheme (AC). The disadvantages lay in the fact that a wavelength does not match standard optical communication, and that efficient bipolar electrical injection has not been yet achieved [13, 28].

*Er coupled to Si nanocrystals in a dielectric.* The demonstrated emission wavelength is  $1.535 \mu\text{m}$ . The system features include internal gain demonstrated in waveguides. The advantages lie in the fact that it is CMOS-compatible and easy to fabricate, in addition to its demonstrated optical cavity and wavelength being suitable for optical communication. The disadvantages lie in the fact that overall gain has not been yet demonstrated in waveguides, and that efficient electrical injection has not been yet achieved [29].

*Strained germanium on Si.* The system's demonstrated emission wavelength is  $1.55 \mu\text{m}$ . The system features are demonstrated by a theory being able to predict high gain. The advantages lie in the fact that

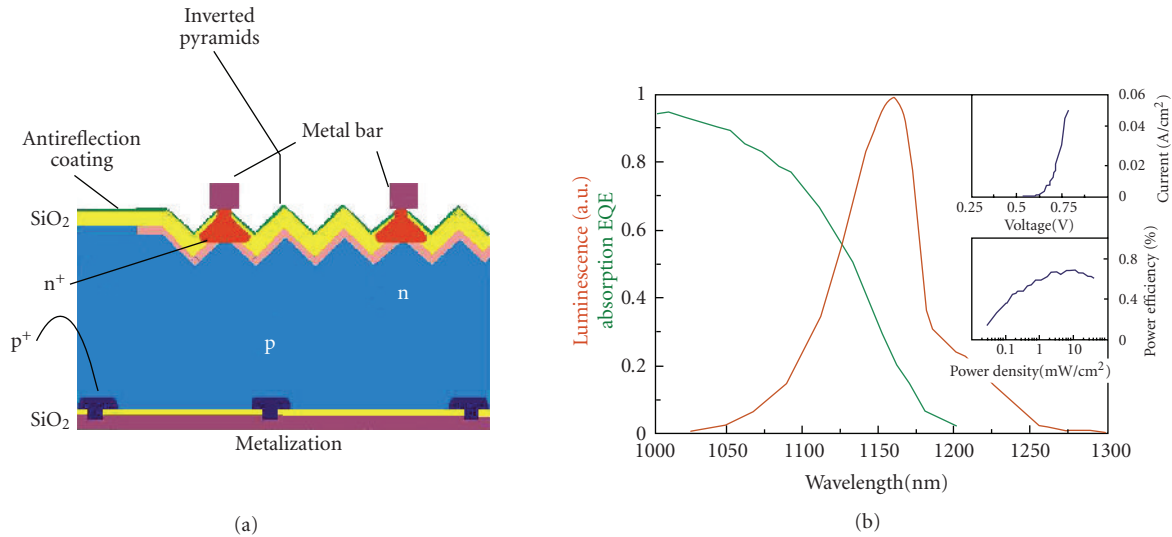


FIGURE 2: Summary of the results of the Australian group on a bulk Si LED. (a) Sketch of the LED geometry. (b) Luminescence spectrum (red), absorption spectrum (green), power efficiency versus injected electrical power density (blue), and I-V characteristics (inset) at room temperature, adapted from [15, 26].

it is easy to fabricate and has a wavelength suitable for optical communication. The disadvantages are manifested by the fact that no experiments are in support of the theory till now [30].

On considering the CMOS compatibility, one should mention that annealing procedure to nucleate the Si nanocrystals requires high temperatures (usually in excess of 1000°C). In a CMOS run, such high-temperature steps can only be introduced at the beginning of the process. This implies that the standard CMOS steps are to be performed after the nanocrystal fabrication. While this is an obviously tight constraint, compatibility with standard CMOS is in principle possible within this limitation. Otherwise one needs to consider other kinds of processing such as layer bonding.

#### 4.1. Bulk Si light-emitting diodes

The common belief that bulk Si cannot be a light-emitting material has been severely questioned in a series of recent works. An Australian group noticed that top-quality solar cells are characterized by extremely long carrier recombination lifetimes of the order of some milliseconds. That is, the recombination lifetime is of the order of the radiative lifetime; hence  $\eta_{\text{int}}$  is of the order of 1. Then, if the solar cell is biased in the forward regime instead of the usual reverse regime, the solar cell could behave as a very efficient light-emitting diode [15, 26].

Figure 2 shows a schematic of the device and a room temperature emission spectrum. To increase the light extraction efficiency, the LED surface was texturized so that most of the internally generated light was impinging on the external surface of the cell with an incident angle lower than the critical angle for total internal refraction. Thus, the light extraction efficiency was increased from a few

% being typical of a flat surface to almost 100% for the texturized LED. Finally, to reduce free-carrier absorption to a minimum, the electrodes, that is, the heavily doped regions, were confined in very thin and small lines. By using these three practices, a plug-in efficiency (ratio of the optical power emitted from the LED to the electrical driving power) larger than 1% at 200 K was achieved. Most interestingly, the turn-on voltage of the device was the same as the forward bias of the solar cell, that is, less than 1 V.

The same research group published also a theoretical paper [31], which questioned one common belief that indirect bandgap materials could not show optical gain because of parasitic absorption processes due to free carriers [32]. Indeed they demonstrated that optical gain is theoretically possible, and pointed out that the most suitable energy region is the sub-bandgap region where processes involving photons could help in achieving gain.

These theoretical arguments have been partially confirmed in a recent study where stimulated emission has been observed (see Figure 3) [33]. As the limit to efficient light generation in Si is the short nonradiative lifetime, the idea was to avoid carrier diffusion and to spatially localize free carriers in a small device region where nonradiative recombination centers can be easily saturated.

Carrier localization was achieved by spin-on doping of small silica nanoparticles at the junction of a p-n diode (Figure 3) [33]. The current-voltage I-V characteristic of the diode shows rectifying behavior with a clear threshold in the light-current L-I characteristic. A change from a broad emission spectrum characteristic of band-to-band emission below threshold to sharp peaks due to stimulated emission above threshold is observed too. Stimulated emission is observed for a two-phonon indirect transition as it was theoretically predicted. Furthermore, when the injection current significantly exceeds the threshold, a single peak dominates. All these results are very encouraging since

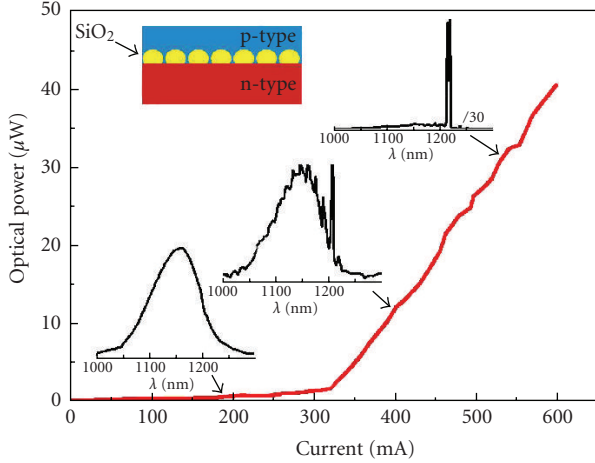


FIGURE 3: Optical power versus injected current for an LED containing  $\text{SiO}_2$  nanoclusters in the junction region (inset). Also shown are a few electroluminescence spectra for different injection rate (arrows), adapted from [33].

the proposed systems have excellent electrical qualities as they are p-n junctions. One puzzling question is about the reproducibility of this work since no other papers were appearing after this result. The crucial question about the nature of the stimulated emission (bulk- or defects-related) is still unanswered.

Recently, another report of stimulated emission in bulk Si has appeared [16]. Nanopatterning of a thin Si on insulator layer allows to have a large effective Si surface, where a sizable density of  $A'$  centers could pile up. These defect centers are believed to play the role of active optical centers which can be optically inverted. Indeed, very convincing experimental data of gain in these nanopatterned films have been reported. The major caveat is that the gain is vanishing as the temperature is raised; sizable gain is observed only for temperatures lower than 80 K.

Strong efficiency improvement of electroluminescence has been independently reported by two groups. They have used carrier confinement in extremely thin Si layers (few nm). In one work [17], lateral  $p^+-p-n^+$  junctions have been developed where the p-layer has been thinned down to 5 nm. Electroluminescence peaked at 1130 nm due to carrier confinement in the thin p-region, and an efficiency of  $1.4 \times 10^{-4}$  was reported ( $0.1 \mu\text{W}$  optical power for mA injection current). In another approach [18, 19], a light-emitting field-effect transistor with lateral p-n junction was used to inject carrier into an active layer made by ultrathin intrinsic Si layer, thinned down using LOCOS processing. Performances similar to the one shown in [17] have been achieved.

#### 4.2. Optical gain in Si nanocrystals

Another interesting approach to form light emitters and amplifiers in Si is to use small Si nanoclusters (Si-nc) dispersed in a dielectric matrix, most frequently  $\text{SiO}_2$  [4]. With this approach, one maximizes carrier confinement, improves the radiative probability by quantum confinement,

shifts the emission wavelength to visible and controls the emission wavelength by Si-nc dimension, decreases the confined carrier absorption due to the decreased emission wavelength, and increases the light extraction efficiency by reducing the dielectric mismatch between the source materials and the air. Various techniques are used to form Si-nc whose size can be tailored in the few nm range (Figure 4).

Starting with an Si rich oxide, which can be formed by deposition, sputtering, ion implantation, cluster evaporation, and so on, a partial phase separation is induced by thermal annealing. The duration of the thermal treatment, the annealing temperature, the starting excess Si content are all determining the final sizes of the clusters, their dispersion in size which can be significant, and the Si-nc crystalline nature. The size dispersion is usually claimed as the source of the broad emission lineshape that at room temperature is typical of the Si-nc emission spectra. In addition to size dispersion, both size-selected deposition [34] and single Si-nc luminescence experiments [35] demonstrate that Si-nc emission is intrinsically broad due to the indirect nature of the emission. The active role of the interface region in determining the optical properties of Si-nc has been highlighted in a joint theoretical and experimental paper [36]. The origin of the luminescence in Si-nc is still unclear; many authors believe that it comes from confined exciton recombination in the Si-nc [37], while others support a defect-assisted recombination mechanism where luminescence is due to recombination of carriers trapped at radiative recombination centers which form at the interface between Si-nc and the dielectric [38] or even in the dielectric [39]. One candidate for these centers is the silanone bond which is formed by double Si-O bonds [40]. The most probable nature of the luminescence in Si-nc is a mechanism which involves both recombination paths: excitons at about 800 nm and trapped carriers on radiative interface state, which form in small sized nanocrystals, at about 700 nm. Indeed, passivation experiments show that the intensity and lineshape of the emission can be influenced by exposition to hydrogen gas or by further oxidation [41].

A number of papers reported observation of optical gain in these systems [13, 42–49]. The observations of gain by several different groups and on several differently prepared materials make the observation solid. Figure 5 reports a summary of the most relevant data taken on Si-nc formed by plasma-enhanced chemical vapor deposition (PECVD) [44, 45, 47]. Two techniques are reported here: the variable stripe length method (VSL) which is sketched in the inset of Figure 5 and is based on the one-dimensional amplifier model [45], and the pump-probe technique which is based on the probe amplification in presence of a high-energy and high-intensity pump beam [47]. In the VSL method, by varying the extent of the pumped region (whose length is  $z$ ), one measures the amplified spontaneous emission ( $I_{\text{ASE}}$ ) signal coming out from an edge of a waveguide whose core is rich in Si-nc:

$$I_{\text{ASE}}(z) = \frac{J_{\text{sp}}(\Omega)}{g_{\text{mod}}} (e^{g_{\text{mod}} z} - 1), \quad (4)$$

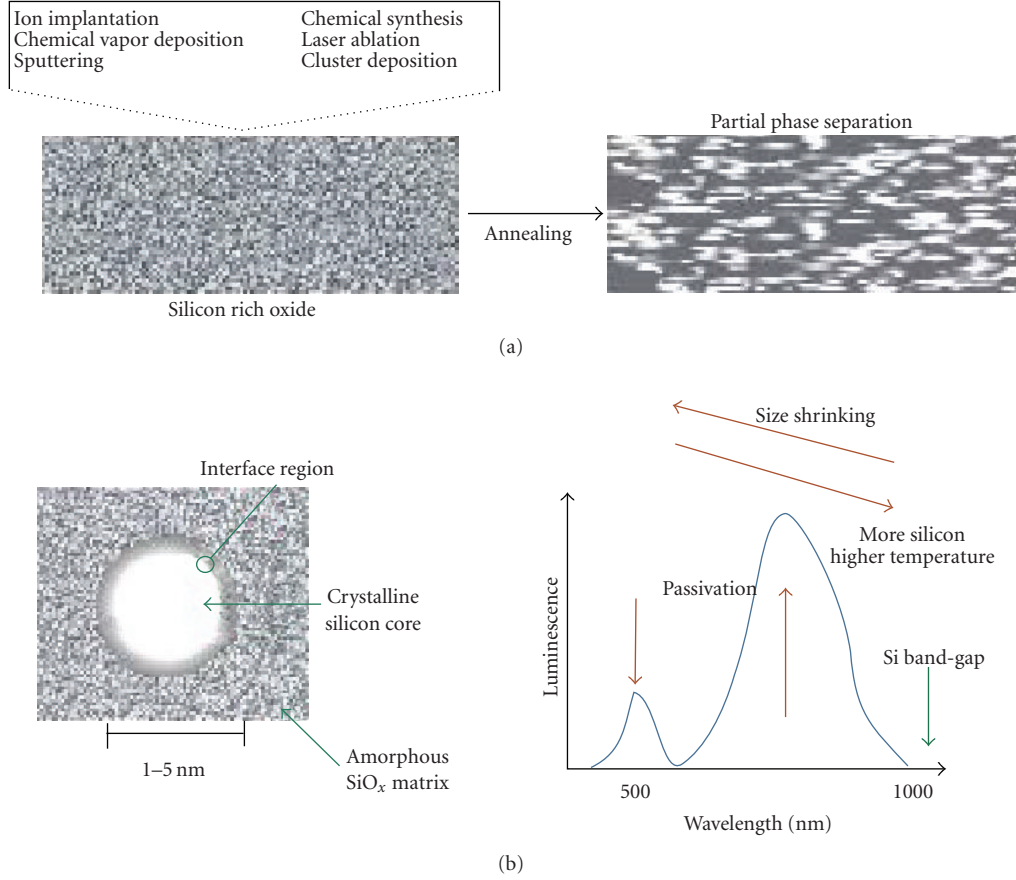


FIGURE 4: Si nanocrystals formation, structure, and luminescence spectrum.

where  $J_{sp}(\Omega)$  is the spontaneous emission intensity emitted within the solid angle  $\Omega$ , and  $g_{mod}$  is the *net modal gain* of the material, defined as  $g_{mod} = \Gamma g_m - \alpha$ .

Data reported in Figure 5 show that the ASE intensity increases sublinearly with the pumping length when the pumping power is lower than a threshold. For pumping power higher than threshold, the ASE signal increases more than exponentially. This is a consequence of the pump-induced switching from absorption ( $g_{mod} < 0$ ) to gain ( $g_{mod} > 0$ ).

In addition, if time-resolved measurements are performed (Figure 5(c)), [45] the ASE decay lineshape shows two time regimes: a fast decay within the first nanosecond, and a slow time decay with typical time constant of few microseconds. It is well known that Si-nc has time decay constant of some microseconds, so the appearance of a nanosecond time decay is at first surprising. What is important is the fact that the fast decay appears only if the pumping power and the excitation volume are both large. If one decreases the excitation volume at high power or the pumping power at large excitation volume, the fast decay disappears. This can be understood if the fast decay is due to stimulated emissions. In fact, at high pumping rate, three competitive paths open: stimulated emission, Auger recombination, and confined carrier absorption. All of these could be the cause of the fast decay. In particular, the Auger

lifetime  $\tau_A$  and the confined carrier absorption lifetime  $\tau_{CC}$  can be modeled in an Si-nc by

$$\tau_A = \frac{1}{C_A N_{ex}}, \quad \tau_{CC} = \frac{1}{2C_{CC} N_{ex}}, \quad (5)$$

where  $C_A$  and  $C_{CC}$  are coefficients, and  $N_{ex}$  is the density of excited recombination centers.  $N_{ex}$  is directly proportional to the pumping power and not to the pumping volume. Thus, by decreasing the pumping length, the ASE lineshape should be unchanged. On the other hand, by a simple rate equation modeling [50], the stimulated emission lifetime  $\tau_{se}$  turns out to be

$$\tau_{se} = \frac{4}{3} \pi (R_{NS})^3 \frac{1}{\xi \sigma_g c n_{ph}}, \quad (6)$$

where  $R_{NS}$  is the average radius of the Si-nc,  $\xi$  is their packing density,  $\sigma_g$  is the gain cross-section, and  $n_{ph}$  is the photon flux density. Note that  $\tau_{se}$  depends not only on the material properties ( $R_{NS}$ ,  $\xi$ ,  $\sigma_g$ ) but also on the photon flux density  $n_{ph}$  which exists in the waveguide. Also,  $n_{ph}$  depends in turn on the waveguide losses, the Si-nc quantum efficiency, and the pumping rates. In addition, if the sample shows gain, by increasing the excitation volume,  $n_{ph}$  exponentially increases; that is,  $\tau_{se}$  decreases.  $\tau_{se}$  shortens when either the pumping length or the pumping power increases as both increase  $n_{ph}$ .

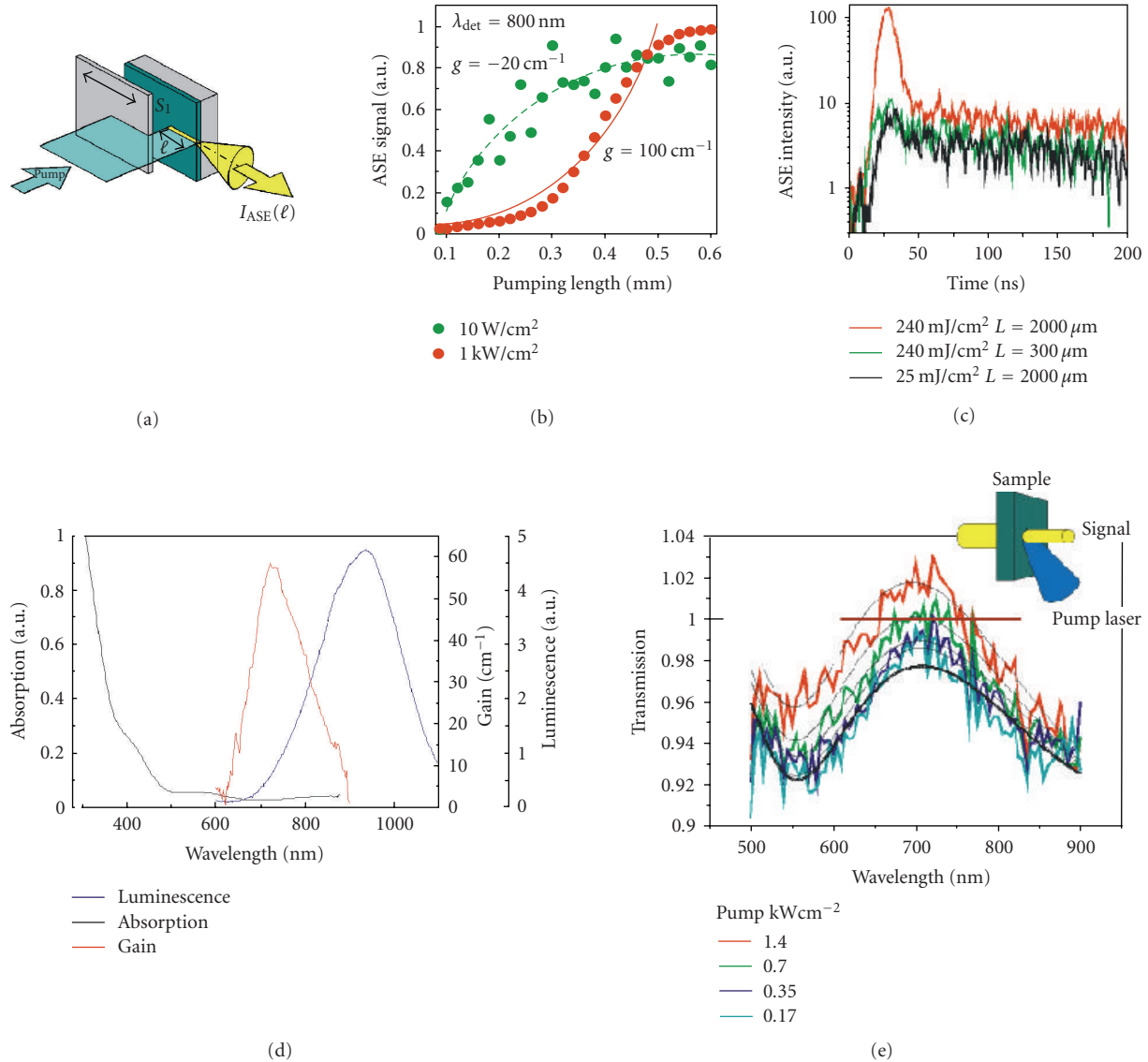


FIGURE 5: Summary of various experimental proofs of gain in Si-nc. (a) Geometry used to measure the amplified spontaneous emission (ASE); (b) ASE versus the pumping length for two pumping powers; (c) ASE time decay for the various pumping conditions indicated in the inset ( $L$  is the pumping length); (d) luminescence, absorption, and gain spectra at room temperature for an Si-nc rich waveguide; (e) transmission spectra for various pumping powers (the inset shows the experimental geometry used). Data have been redrawn from [44, 45, 47].

It is important to note that calculations show that the Auger lifetime in Si-nc is in the interval of 0.1–10 nanoseconds [51], which means that Auger recombination is a strong competitive process which should be always considered. In some Si-nc systems, due to either material problems or poor waveguide properties or even both, Auger recombination and confined carrier absorption might prevail, and no optical gain could be observed.

Figure 5(d) shows a summary of the wavelength dependence of the luminescence, absorption, and gain spectra in a sample with 4 nm Si-nc [44]. It is seen that the gain spectrum is on the high-energy side of the emission band and that absorption is negligible in the region of gain and luminescence. These facts suggest a four-level model to

explain the gain where the levels can be associated with both different Si-nc populations or with a radiative state associated with an Si=O double bond for which optical excitation causes a large lattice relaxation of the Si=O bond [52, 53] as in the silanone molecule. A recent paper shows that oxide is needed to observe gain [54]. Indeed, Si nanocrystals formed in Si nitride do not show gain, while Si nanocrystals formed in Si oxide do show gain.

Pump-probe measurements were attempted with contradictory results [47, 55]. Our group was able to show probe amplification under pumping conditions (see Figure 5(e)) [47], while another group reported pump-induced absorption probably associated with confined carrier absorption [55]. Literature results show that the confined carrier

absorption cross-section  $\sigma_{fc}$  in Si-nc is at least one order of magnitude reduced with respect to bulk Si [56]:  $\sigma_{fc} \approx 10^{-18} \text{ cm}^2$  at  $1.55 \mu\text{m}$  in P-doped Si-nc. This cross-section should be further reduced at  $700 \text{ nm}$  due to the  $\lambda^2$  dependence of the confined carrier absorption. Transmission measurements of a probe beam through an Si-nc slab deposited on a quartz substrate show the typical interference fringes due to multiple reflection at the slab interfaces (Figure 5). When the pump power is raised, the transmission is increased and, at the maximum power used, net probe amplification with respect to the input probe intensity in air is observed in a narrow wavelength interval. Note that the probe amplification spectrum overlaps the fast luminescence spectrum measured by time-resolved technique. Based on these results, design of optical cavity for an Si-nc laser has been published [57].

In addition, very favorable results have been published with respect to Si-nc-based LED, where turn-on voltage as low as few volts can be demonstrated by using thin Si-nc active layers [58]. Electroluminescence in these LEDs was due to impact excitation of electron-hole pairs in the Si-nc. Improvements in the electroluminescence efficiency have been achieved by using Si nanocrystals dispersed within a polymer matrix [59].

Another recent work reports on an FET structure where the gate dielectric is rich in Si-nc [28]. In this way, by changing the sign of the gate bias, separate injection of electrons and holes in the Si-nc is achieved. Luminescence is observed only when both electrons and holes are injected into the Si-nc. By using this pulsing bias technique, high efficiency in the emission of the LED is achieved due to the copresence of electrons and holes. Channel optical waveguide with a core layer rich in Si-nc shows optical losses of only a few dB/cm mainly due to direct Si-nc absorption and to scattering caused by the composite nature of the guiding medium [60]. All these different experiments have still to be merged into a laser cavity structure to demonstrate an Si-nc-based laser.

### 4.3. Light amplification in Er-coupled Si nanoclusters

The radiative transitions in the internal 4f shell of erbium ions ( $\text{Er}^{3+}$ ) are exploited in the erbium-doped fiber amplifier (EDFA) [61], an all optical amplifier which has revolutionized the optical communication technology. During the nineties, several experimental efforts have been exerted in order to develop an efficient and reliable light source by using  $\text{Er}^{3+}$  in Si [4]. The idea was to excite the  $\text{Er}^{3+}$ , which emits  $1.535 \mu\text{m}$  photons, by an energy transfer from the electrically injected e-h pairs in a p-n Si diode. The most successful results have been shown by the demonstration of room temperature emission with an external quantum efficiency of 0.1% in an MHz modulated  $\text{Er}^{3+}$ -doped Si LED [62]. The main problem associated with  $\text{Er}^{3+}$  in Si is the back transfer of energy from the  $\text{Er}^{3+}$  ions to the Si host, which causes a lowering of the emission efficiency of the diode [63]. This is due to a resonant level which appears in the Si bandgap due to the  $\text{Er}^{3+}$  doping and which couples with the  $\text{Er}^{3+}$  levels. In order to reduce this back-transfer process, it was proposed to

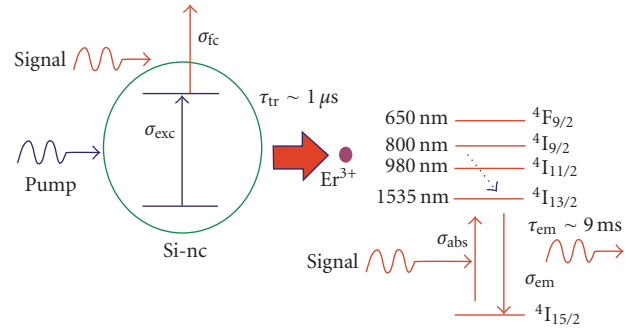


FIGURE 6: Diagram of the excitation process of  $\text{Er}^{3+}$  ions via an Si-nc, with the main related cross-sections. On the right, the main internal energy levels of the  $\text{Er}^{3+}$  are shown.

enlarge the bandgap of the  $\text{Er}^{3+}$  host so that the resonance between the defect level and the internal  $\text{Er}^{3+}$  levels is lost [64]. Si-nc in an  $\text{SiO}_2$  dielectric were thus proposed as the host [65]. Indeed, it turns out that Si-nc are very efficient sensitizers of the  $\text{Er}^{3+}$  luminescence with typical transfer efficiency as high as 70% and with a typical transfer time of 1 microsecond [66]. In addition, the  $\text{Er}^{3+}$  are dispersed in  $\text{SiO}_2$ , where they found their most favorable chemical environment. Quite interestingly, the transfer efficiency gets maximized when the Si-nc are not completely crystallized but still in the form of Si nanoclusters [67]. Some reports claim even that the  $\text{Er}^{3+}$  can be excited through defects in the matrix [68]. Still under debate is the number of Er ions that can be excited by a single Si-nc: a few or many ions.

Figure 6 summarizes the various mechanisms, and defines the related cross-sections for this system. Excitation of  $\text{Er}^{3+}$  occurs via an energy transfer from photoexcited e-h pairs which are excited in the Si-nc; the overall efficiency of light generation at  $1.535 \mu\text{m}$  through direct absorption in the Si-nc is described by an effective  $\text{Er}^{3+}$  excitation cross-section  $\sigma_{\text{exc}}$ . On the other hand, the direct absorption of the  $\text{Er}^{3+}$  ions, without the mediation of the Si-nc, and the emission from the Er ions are described by absorption  $\sigma_{\text{abs}}$  and emission  $\sigma_{\text{em}}$  cross-sections, respectively. The typical radiative lifetime of  $\text{Er}^{3+}$  is of the order of 1 millisecond, with values as high as 7 milliseconds in carefully prepared samples, which is similar to the one of  $\text{Er}^{3+}$  in pure  $\text{SiO}_2$  [69]. Figure 7(a) reports the luminescence and absorption spectra measured in an  $\text{Er}^{3+}$ -coupled Si-nc ridge waveguide at room temperature [70, 71].

Table 1 summarizes the results for the various cross-sections which are the results of an intensive study [72]. It is important to note the five orders of magnitude increase in  $\sigma_{\text{exc}}$  and the fact that this value is conserved also when electrical injection is used to excite the Si-nc [73]. If one places the  $\text{Er}^{3+}$  ions in an Si-nc ridge waveguide (see inset of Figure 7(b)), one can perform experiments on signal amplification at  $1.535 \mu\text{m}$  with the aim of demonstrating an Er-doped waveguide amplifier (EDWA). The main advantage of an EDWA with respect to an EDFA is the reduced size, the decreased pump power to achieve the same gain, and the

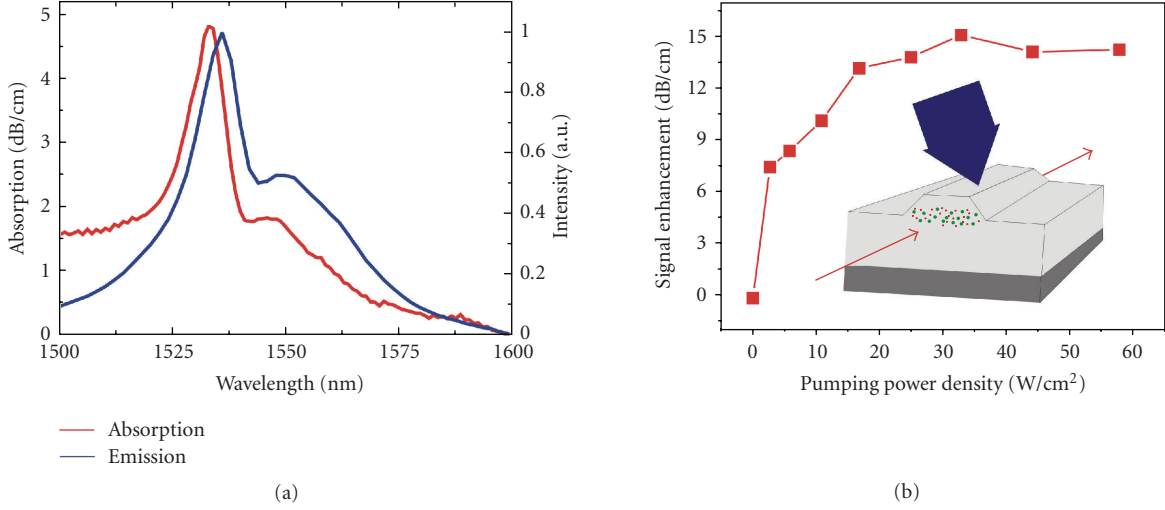


FIGURE 7: (a) Absorption and luminescence spectra of an  $\text{Er}^{3+}$ -coupled Si-nc waveguide. Adapted from [71]. (b) Signal enhancement at  $1.535 \mu\text{m}$  in an  $\text{Er}^{3+}$ -coupled Si-nc waveguide versus the pumping power density by using top pumping as shown in the inset. Adapted from [74].

TABLE 1: Summary of the various cross-sections related to  $\text{Er}^{3+}$  coupled to Si-nc. These values are the results of the LANCER collaboration [71].

Erbium absorption cross-section at 1530 nm	$\sigma_{\text{abs}} = 6.6 \times 10^{-21} \text{ cm}^2$
Erbium emission cross-section at 1530 nm	$\sigma_{\text{em}} = 5.7 \times 10^{-21} \text{ cm}^2$
Erbium effective cross-section at 470 nm	$\sigma_{\text{exc}} = 2 \times 10^{-16} \text{ cm}^2$
Erbium metastable level lifetime	3 ms
Erbium decay time ${}^4I_{11/2}$ to ${}^4I_{13/2}$ transition	2.38 $\mu\text{s}$
Upconversion coefficient $C_{\text{up}}$ for $N_{\text{Er}} < 3 \times 10^{20} \text{ cm}^{-3}$	$7 \times 10^{-17} \text{ cm}^3/\text{s}$
Si-nc absorption cross-section at 470 nm	$\sigma_{\text{Si}} = 2 \times 10^{-16} \text{ cm}^2$
Si-nc exciton lifetime $\tau_{\text{ab}}$	50 $\mu\text{s}$
Transfer coefficient	$C_{b1} = 2 \times 10^{-15} \text{ cm}^3/\text{s}$

wide spectrum range to optically pump the system. A few groups have performed such an experiment [70, 71, 74–76].

The most successful result was reported in [76] (see Figure 7(b)). In this work, a very low Si-nc concentration has been used, and an internal gain of 7 dB/cm has been deduced. A successful experiment of pumping the EDWA with LED was also reported [76]. In other experiments, with a large Si-nc concentration, no or weak signal enhancement has been observed [70, 71, 75]. The reason is attributed to the presence of a strong confined carrier absorption which introduces a loss mechanism at the signal wavelength, and prevents the sensitizing action of the Si-nc. Indeed, the energy transfer is in competition with confined carrier absorption at the signal wavelength (see Figure 6). A confined carrier cross-section of  $10^{-18} \text{ cm}^2$  is usually assumed [66]. Propagation losses, saturation of  $\text{Er}^{3+}$  excitation, upconversion, and confined carrier absorption make the proper design of EDWA difficult, where optical amplification can be observed. The most relevant problem in the realization of an amplifier is related to the fact that the coupling of Er with Si-nc is not complete. Indeed, most of the reported works show that only up to 5%

of the Er ions are coupled to the Si-nc, while the other can be excited only through direct Er absorption [72]. This is the main problem limiting the achievement of a net overall gain in the waveguide amplifier. In addition, a flux-dependent effective excitation cross-section has been demonstrated due to the distance-dependent coupling coefficient. Higher flux yields lower excitation cross-section due to the saturation of the strongly coupled ions. Thus, the main problem to obtain overall gain with this system concerns the nanoengineering of the material composition, allowing the production of materials with a high density of small sized Si-nc coupled effectively to all the Er ions in the system. The small size is needed to minimize the confined carrier absorption, while the high density is necessary to increase the coupling with the Er ions [72]. Having obtained internal gain, electrically injected LED [63, 77], and optical cavities [78], a laser which uses the  $\text{Er}^{3+}$ -coupled Si-nc system as active material seems feasible. With this respect, it is worth noticing that toroidal microcavities formed in silica doped with  $\text{Er}^{3+}$  have demonstrated optically pumped lasing at room temperature [79].

## 5. CONCLUSIONS

After seven years from the first observation of optical gain in Si nanocrystals, a first Si laser has been demonstrated, though not using Si-nc but the Raman effect. Various different approaches have been however suggested to achieve electrically pumped lasing in Si. These cover a wide spectral range from visible to infrared. These facts show that the perspectives to achieve an injection laser in Si are nowadays more solid than ever. We are quite optimistic that a laser will be realized in the near future by using one of the various approaches presented here.

## ACKNOWLEDGMENTS

The collaboration with the MTLab of FBK-irst (Dr. Bellutti and Dr. Pucker) has allowed us to reach a detailed view of the field. The supports of EC (LANCER: FP6-033574; PHOLOGIC: FP6-017158), INTEL, and PAT are gratefully acknowledged.

## REFERENCES

- [1] S. S. Iyer and Y.-H. Xie, "Light emission from silicon," *Science*, vol. 260, no. 5104, pp. 40–46, 1993.
- [2] L. C. Kimerling, K. D. Kolenbrander, J. Michel, and J. Palm, "Light emission from silicon," *Solid State Physics*, vol. 50, p. 333, 1997.
- [3] O. Bisi, S. U. Campisano, L. Pavesi, and F. Priolo, *Silicon-Based Microphotonics, From Basics to Applications*, IOS Press, Amsterdam, The Netherlands, 1999.
- [4] S. Ossicini, L. Pavesi, and F. Priolo, *Light Emitting Silicon for Microphotonics*, Springer, Berlin, Germany, 2003.
- [5] L. Pavesi, S. Gaponenko, and L. Dal Negro, *Towards the First Silicon Laser*, NATO Science, Kluwer Academic Publishers, Dordrecht, The Netherlands, 2003.
- [6] G. Reed and A. Knights, *Silicon Photonics: An Introduction*, John Wiley & Sons, New York, NY, USA, 2004.
- [7] L. Pavesi and D. Lockwood, *Silicon Photonics, Vol. 94 of Topics in Applied Physics*, Springer, Berlin, Germany, 2004.
- [8] L. Pavesi and G. Guillot, *Optical Interconnects: The Silicon Route*, Springer, Berlin, Germany, 2006.
- [9] "Shining light on Silicon," *Materials Today*, vol. 10, no. 7-8, 2007.
- [10] O. Svelto, *Principles of Lasers*, Springer, Berlin, Germany, 4th edition, 1998.
- [11] W. S. C. Chang, *Principles of Lasers and Optics*, Cambridge University Press, Cambridge, UK, 2005.
- [12] P. Jonsson, H. Bleichner, M. Isberg, and E. Nordlander, "The ambipolar Auger coefficient: measured temperature dependence in electron irradiated and highly injected n-type silicon," *Journal of Applied Physics*, vol. 81, no. 5, pp. 2256–2262, 1997.
- [13] L. Pavesi, L. Dal Negro, C. Mazzoleni, G. Franzò, and F. Priolo, "Optical gain in silicon nanocrystals," *Nature*, vol. 408, pp. 440–444, 2000.
- [14] G. Dehlinger, L. Diehl, U. Gennser, et al., "Intersubband electroluminescence from silicon-based quantum cascade structures," *Science*, vol. 290, no. 5500, pp. 2277–2280, 2000.
- [15] M. A. Green, J. Zhao, A. Wang, P. J. Reece, and M. Gal, "Efficient silicon light-emitting diodes," *Nature*, vol. 412, no. 6849, pp. 805–808, 2001.
- [16] S. G. Cloutier, P. A. Kosyrev, and J. Xu, "Optical gain and stimulated emission in periodic nanopatterned crystalline silicon," *Nature Materials*, vol. 4, no. 12, pp. 887–891, 2005.
- [17] T. Hoang, P. LeMinh, J. Holleman, and J. Schmitz, "Strong efficiency improvement of SOI-LEDs through carrier confinement," *IEEE Electron Device Letters*, vol. 28, no. 5, pp. 383–385, 2007.
- [18] S.-I. Saito, D. Hisamoto, H. Shimizu, et al., "Silicon light-emitting transistor for on-chip optical interconnection," *Applied Physics Letters*, vol. 89, no. 16, Article ID 163504, 3 pages, 2006.
- [19] S.-I. Saito, D. Hisamoto, H. Shimizu, et al., "Electroluminescence from ultra-thin silicon," *Japanese Journal of Applied Physics*, vol. 45, pp. L679–L682, 2006.
- [20] R. Claps, D. Dimitropoulos, V. Raghunathan, Y. Han, and B. Jalali, "Observation of stimulated Raman amplification in silicon waveguides," *Optics Express*, vol. 11, no. 15, pp. 1731–1739, 2003.
- [21] O. Boyraz and B. Jalali, "Demonstration of a silicon Raman laser," *Optics Express*, vol. 12, no. 21, pp. 5269–5273, 2004.
- [22] O. Boyraz and B. Jalali, "Demonstration of directly modulated silicon Raman laser," *Optics Express*, vol. 13, no. 3, pp. 796–800, 2005.
- [23] A. Liu, H. Rong, M. Paniccia, O. Cohen, and D. Hak, "Net optical gain in a low loss silicon-on-insulator waveguide by stimulated Raman scattering," *Optics Express*, vol. 12, no. 18, pp. 4261–4268, 2004.
- [24] H. Rong, A. Liu, R. Jones, et al., "An all-silicon Raman laser," *Nature*, vol. 433, no. 7023, pp. 292–294, 2005.
- [25] H. Rong, R. Jones, A. Liu, et al., "A continuous-wave Raman silicon laser," *Nature*, vol. 433, no. 7027, pp. 725–728, 2005.
- [26] J. Zhao, M. A. Green, and A. Wang, "High-efficiency optical emission, detection, and coupling using silicon diodes," *Journal of Applied Physics*, vol. 92, no. 6, pp. 2977–2979, 2002.
- [27] W. L. Ng, M. A. Lourenço, R. M. Gwilliam, S. Ledain, G. Shao, and K. P. Homewood, "An efficient room-temperature silicon-based light-emitting diode," *Nature*, vol. 410, no. 6825, pp. 192–194, 2001.
- [28] R. J. Walters, G. I. Bourianoff, and H. A. Atwater, "Field-effect electroluminescence in silicon nanocrystals," *Nature Materials*, vol. 4, no. 2, pp. 143–146, 2005.
- [29] N. Daldosso, D. Navarro-Urrios, M. Melchiorri, et al., "Er-coupled Si nanocluster waveguide," *IEEE Journal on Selected Topics in Quantum Electronics*, vol. 12, no. 6, pp. 1607–1617, 2006.
- [30] J. Liu, X. Sun, D. Pan, et al., "Tensile-strained, n-type Ge as a gain medium for monolithic laser integration on Si," *Optics Express*, vol. 15, no. 18, pp. 11272–11277, 2007.
- [31] T. Trupke, M. A. Green, and P. Würfel, "Optical gain in materials with indirect transitions," *Journal of Applied Physics*, vol. 93, no. 11, pp. 9058–9061, 2003.
- [32] W. P. Dumke, "Interband transitions and maser action," *Physical Review*, vol. 127, no. 5, pp. 1559–1563, 1962.
- [33] M. J. Chen, J. L. Yen, J. Y. Li, J. F. Chang, S. C. Tsai, and C. S. Tsai, "Stimulated emission in a nanostructured silicon pn junction diode using current injection," *Applied Physics Letters*, vol. 84, no. 12, pp. 2163–2165, 2004.
- [34] M. Zacharias, J. Heitmann, R. Scholz, U. Kahler, M. Schmidt, and J. Blasing, "Size-controlled highly luminescent silicon nanocrystals: a SiO/SiO<sub>2</sub> superlattice approach," *Applied Physics Letters*, vol. 80, no. 4, pp. 661–663, 2002.
- [35] J. Valenta, R. Juhasz, and J. Linnros, "Photoluminescence spectroscopy of single silicon quantum dots," *Applied Physics Letters*, vol. 80, no. 6, pp. 1070–1072, 2002.

- [36] N. Dalbosso, M. Luppi, S. Ossicini, et al., "Role of the interface region on the optoelectronic properties of silicon nanocrystals embedded in SiO<sub>2</sub>," *Physical Review B*, vol. 68, no. 8, Article ID 085327, 8 pages, 2003.
- [37] J. Heitmann, F. Müller, L. Yi, M. Zacharias, D. Kovalev, and F. Eichhorn, "Excitons in Si nanocrystals: confinement and migration effects," *Physical Review B*, vol. 69, no. 19, Article ID 195309, 7 pages, 2004.
- [38] L. Khriachtchev, M. Räsänen, S. Novikov, O. Kilpelä, and J. Sinkkonen, "Raman scattering from very thin Si layers of SiO/SiO<sub>2</sub> superlattices: experimental evidence of structural modification in the 0.8–3.5 nm thickness region," *Journal of Applied Physics*, vol. 86, no. 10, pp. 5601–5608, 1999.
- [39] L. Khriachtchev, M. Räsänen, S. Novikov, and L. Pavesi, "Systematic correlation between Raman spectra, photoluminescence intensity, and absorption coefficient of silica layers containing Si nanocrystals," *Applied Physics Letters*, vol. 85, no. 9, pp. 1511–1513, 2004.
- [40] Y. J. Chabal, K. Raghavachari, X. Zhang, and E. Garfunkel, "Silanone (Si=O) on Si(100): intermediate for initial silicon oxidation," *Physical Review B*, vol. 66, no. 16, Article ID 161315, 4 pages, 2002.
- [41] J. S. Biteen, N. S. Lewis, H. A. Atwater, and A. Polman, "Size-dependent oxygen-related electronic states in silicon nanocrystals," *Applied Physics Letters*, vol. 84, no. 26, pp. 5389–5391, 2004.
- [42] L. Khriachtchev, M. Räsänen, S. Novikov, and J. Sinkkonen, "Optical gain in SiO/SiO<sub>2</sub> lattice: experimental evidence with nanosecond pulses," *Applied Physics Letters*, vol. 79, no. 9, pp. 1249–1251, 2001.
- [43] M. H. Nayfeh, S. Rao, N. Barry, et al., "Observation of laser oscillation in aggregates of ultrasmall silicon nanoparticles," *Applied Physics Letters*, vol. 80, no. 1, pp. 121–123, 2002.
- [44] L. Dal Negro, M. Cazzanelli, N. Dalbosso, et al., "Stimulated emission in plasma-enhanced chemical vapour deposited silicon nanocrystals," *Physica E*, vol. 16, no. 3-4, pp. 297–308, 2003.
- [45] L. Dal Negro, M. Cazzanelli, L. Pavesi, et al., "Dynamics of stimulated emission in silicon nanocrystals," *Applied Physics Letters*, vol. 82, no. 26, pp. 4636–4638, 2003.
- [46] J. Ruan, P. M. Fauchet, L. Dal Negro, M. Cazzanelli, and L. Pavesi, "Stimulated emission in nanocrystalline silicon superlattices," *Applied Physics Letters*, vol. 83, no. 26, pp. 5479–5481, 2003.
- [47] L. Dal Negro, M. Cazzanelli, B. Danese, et al., "Light amplification in silicon nanocrystals by pump and probe transmission measurements," *Journal of Applied Physics*, vol. 96, no. 10, pp. 5747–5755, 2004.
- [48] M. Cazzanelli, D. Kovalev, L. Dal Negro, Z. Gaburro, and L. Pavesi, "Polarized optical gain and polarization-narrowing of heavily oxidized porous silicon," *Physical Review Letters*, vol. 93, no. 20, Article ID 207402, 4 pages, 2004.
- [49] K. Luterová, K. Dohnalová, V. Švrček, et al., "Optical gain in porous silicon grains embedded in sol-gel derived SiO<sub>2</sub> matrix under femtosecond excitation," *Applied Physics Letters*, vol. 84, no. 17, pp. 3280–3282, 2004.
- [50] V. I. Klimov, A. A. Mikhailovsky, S. Xu, et al., "Optical gain and stimulated emission in nanocrystal quantum dots," *Science*, vol. 290, no. 5490, pp. 314–317, 2000.
- [51] C. Delerue, M. Lannoo, G. Allan, et al., "Auger and coulomb charging effects in semiconductor nanocrystallites," *Physical Review Letters*, vol. 75, no. 11, pp. 2228–2231, 1995.
- [52] F. Zhou and J. D. Head, "Role of Si=O in the photoluminescence of porous silicon," *Journal of Physical Chemistry*, vol. 104, no. 43, pp. 9981–9986, 2000.
- [53] A. B. Filonov, S. Ossicini, F. Bassani, and F. Arnaud d'Avitaya, "Effect of oxygen on the optical properties of small silicon pyramidal clusters," *Physical Review B*, vol. 65, no. 19, Article ID 195317, 9 pages, 2002.
- [54] H. Chen, J. H. Shin, P. M. Fauchet, J.-Y. Sung, J.-H. Shin, and G. Y. Sung, "Ultrafast photoluminescence dynamics of nitride-passivated silicon nanocrystals using the variable stripe length technique," *Applied Physics Letters*, vol. 91, no. 17, Article ID 173121, 3 pages, 2007.
- [55] R. G. Elliman, M. J. Lederer, N. Smith, and B. Luther-Davies, "The fabrication and properties of silicon-nanocrystal-based devices and structures produced by ion implantation—the search for gain," *Nuclear Instruments and Methods in Physics Research Section B*, vol. 206, pp. 427–431, 2003.
- [56] A. Mimura, M. Fujii, S. Hayashi, D. Kovalev, and F. Koch, "Photoluminescence and free-electron absorption in heavily phosphorus-doped Si nanocrystals," *Physical Review B*, vol. 62, no. 19, pp. 12625–12627, 2000.
- [57] S. L. Jaiswal, J. T. Simpson, S. P. Withrow, C. W. White, and P. M. Norris, "Design of a nanoscale silicon laser," *Applied Physics A*, vol. 77, no. 1, pp. 57–61, 2003.
- [58] G. Franzò, A. Irrera, E. C. Moreira, et al., "Electroluminescence of silicon nanocrystals in MOS structures," *Applied Physics A*, vol. 74, no. 1, pp. 1–5, 2002.
- [59] R. K. Ligan, L. Mangolini, U. R. Kortshagen, and S. A. Campbell, "Electroluminescence from surface oxidized silicon nanoparticles dispersed within a polymer matrix," *Applied Physics Letters*, vol. 90, no. 6, Article ID 061116, 3 pages, 2007.
- [60] P. Pellegrino, B. Garrido, C. Garcia, et al., "Low-loss rib waveguides containing Si nanocrystals embedded in SiO<sub>2</sub>," *Journal of Applied Physics*, vol. 97, no. 7, Article ID 074312, 8 pages, 2005.
- [61] E. Desurvire, *Erbium-Doped Fiber Amplifiers: Principles and Applications*, John Wiley & Sons, New York, NY, USA, 1994.
- [62] G. Franzò, S. Coffa, F. Priolo, and C. Spinella, "Mechanism and performance of forward and reverse bias electroluminescence at 1.54 μm from Er-doped Si diodes," *Journal of Applied Physics*, vol. 81, no. 6, pp. 2784–2793, 1997.
- [63] F. Priolo, G. Franzò, S. Coffa, and A. Carnera, "Excitation and nonradiative deexcitation processes of Er<sup>3+</sup> in crystalline Si," *Physical Review B*, vol. 57, no. 8, pp. 4443–4455, 1998.
- [64] A. J. Kenyon, P. F. Trwoga, M. Federighi, and C. W. Pitt, "Optical properties of PECVD erbium-doped silicon-rich silica: evidence for energy transfer between silicon microclusters and erbium ions," *Journal of Physics: Condensed Matter*, vol. 6, no. 21, pp. L319–L324, 1994.
- [65] M. Fujii, M. Yoshida, Y. Kanzawa, S. Hayashi, and K. Yamamoto, "1.54 μm photoluminescence of Er<sup>3+</sup> doped into SiO<sub>2</sub> films containing Si nanocrystals: evidence for energy transfer from Si nanocrystals to Er<sup>3+</sup>," *Applied Physics Letters*, vol. 71, no. 9, pp. 1198–1200, 1997.
- [66] D. Pacifici, G. Franzò, F. Priolo, F. Iacona, and L. Dal Negro, "Modeling and perspectives of the Si nanocrystals-Er interaction for optical amplification," *Physical Review B*, vol. 67, no. 24, Article ID 245301, 13 pages, 2003.
- [67] G. Franzò, S. Boninelli, D. Pacifici, F. Priolo, F. Iacona, and C. Bongiorno, "Sensitizing properties of amorphous Si clusters on the 1.54-μm luminescence of Er in Si-rich SiO<sub>2</sub>," *Applied Physics Letters*, vol. 82, no. 22, pp. 3871–3873, 2003.

- [68] D. Kuritsyn, A. Kozanecki, H. Przybylińska, and W. Jantsch, "Defect-mediated and resonant optical excitation of  $\text{Er}^{3+}$  ions in silicon-rich silicon oxide," *Applied Physics Letters*, vol. 83, no. 20, pp. 4160–4162, 2003.
- [69] M. Wojdak, M. Klik, M. Forcales, et al., "Sensitization of Er luminescence by Si nanoclusters," *Physical Review B*, vol. 69, no. 23, Article ID 233315, 4 pages, 2004.
- [70] N. Daldosso, D. Navarro-Urrios, M. Melchiorri, et al., "Absorption cross section and signal enhancement in Er-doped Si nanocluster rib-loaded waveguides," *Applied Physics Letters*, vol. 86, no. 26, Article ID 261103, 3 pages, 2005.
- [71] N. Daldosso, D. Navarro-Urrios, M. Melchiorri, et al., "Refractive index dependence of the absorption and emission cross sections at  $1.54 \mu\text{m}$  of  $\text{Er}^{3+}$  coupled to Si nanoclusters," *Applied Physics Letters*, vol. 88, no. 16, Article ID 161901, 3 pages, 2006.
- [72] V. Toccafondo, F. Di Pasquale, S. Faralli, N. Daldosso, L. Pavesi, and H. E. Hernandez-Figueroa, "Study of an efficient longitudinal multimode pumping scheme for Si-nc sensitized EDWAs," *Optics Express*, vol. 15, no. 22, pp. 14907–14913, 2007.
- [73] F. Priolo, G. Franzò, D. Pacifici, V. Vinciguerra, F. Iacona, and A. Irrera, "Role of the energy transfer in the optical properties of undoped and Er-doped interacting Si nanocrystals," *Journal of Applied Physics*, vol. 89, no. 1, pp. 264–272, 2001.
- [74] H.-S. Han, S.-Y. Seo, J. H. Shin, and N. Park, "Coefficient determination related to optical gain in erbium-doped silicon-rich silicon oxide waveguide amplifier," *Applied Physics Letters*, vol. 81, no. 20, pp. 3720–3722, 2002.
- [75] P. G. Kik and A. Polman, "Gain limiting processes in Er-doped Si nanocrystal waveguides in  $\text{SiO}_2$ ," *Journal of Applied Physics*, vol. 91, no. 1, pp. 534–536, 2002.
- [76] J. Lee, J. Shin, and N. Park, "Optical gain in Si-nanocrystal sensitized, Er-doped silica waveguide using top-pumping 470 nm LED," in *Proceedings of Optical Fiber Communication Conference*, Los Angeles, Calif, USA, February 2004.
- [77] M. E. Castagna, S. Coffa, M. Monaco, et al., "High efficiency light emitting devices in silicon," *Materials Science and Engineering: B*, vol. 105, no. 1–3, pp. 83–90, 2003.
- [78] F. Iacona, G. Franzò, E. C. Moreira, and F. Priolo, "Silicon nanocrystals and  $\text{Er}^{3+}$  ions in an optical microcavity," *Journal of Applied Physics*, vol. 89, no. 12, pp. 8354–8356, 2001.
- [79] A. Polman, B. Min, J. Kalkman, T. J. Kippenberg, and K. J. Vahala, "Ultralow-threshold erbium-implanted toroidal microlaser on silicon," *Applied Physics Letters*, vol. 84, no. 7, pp. 1037–1039, 2004.